

Satellite-Based Land Surface Temperature Estimation of Bogor Municipality, Indonesia

Ema Kurnia^{*1}, I Nengah Surati Jaya², Widiatmaka³

¹Department of Master of Science in Information Technology for Natural Resources Management, Faculty of Mathematic and Natural Science, Bogor Agricultural University

²Department of Forest Management, Faculty of Forestry, Bogor Agricultural University

³Department of Soil Science and Land Resources, Faculty of Agriculture, Bogor Agricultural University

*Correspondence author: emakurnia@gmail.com¹, ins-jaya@ipb.ac.id², widiatmaka@yahoo.com³

Abstract

The earth's average temperature has been a big issue on the global warming. The warming of the earth is largely the results of emission of carbon dioxide and other greenhouse gasses (GHG) from human activities. As a hinterland of the Capital City, in the last two decades, Bogor is also getting warmer in comparison with the previous decades. This paper presents how the land surface temperature (LST) had been estimated using Split-Window (SW) algorithm and how its spatial distribution in Bogor Municipality was computed. The spectral radiance of Landsat-8 TIR bands 10 and 11, the emissivity values, and water vapor used as the input on SW Algorithm. The study revealed that the temperature within the built-up area, have warmer temperature than their surrounding ranging from 40°C to 45°C of 3,403.9 ha. The use of SW algorithm is quite reliable and accurate to estimate the LST derived from Landsat-8 having a mean deviation of only 2.7%, less than standard acceptable of 10%.

Keywords: LST, SW Algorithm, TIR

Copyright © 2016 Institute of Advanced Engineering and Science. All rights reserved.

1. Introduction

Now, the global warming has been an international issue that attracting the international attention. At the site level, the land surface temperature (LST) has been used by many researchers as an indicator of energy balance. Specifically, the LST has been used as a key parameter that describes the land surface processes. Within the urban areas, the LST might be closely related to the urban heat island (UHI) which is mainly affected by the human activities. The causes of UHI mainly comes from the human activities that include lifestyle, that use fossil fuel in main human activities, e.g., liquid petroleum gasses for cooking, electricity for room heating and cooling, gasoline or diesel for transportation, industry etc. The waste from the energy usage by every household was also a secondary contributor to the heat. As the population in the city also grows, this tends to expand the area and increase its average temperature. Development of built-up area with the less green open area may cause global temperature changes that result in a change of climate elements, especially the increase in temperature.

The UHI extent may vary across a city, depending on the spatial distribution of the green house gasses (GHG) emitter and absorber. Tahareported that heat islands can develop in 'pockets' around single buildings and temperature differences of 4 °C have been reported along a single street [1]. It is also mentioned that the UHI is affected by the height and spacing of buildings and their orientation relative to the prevailing wind that restrict airflow and limit cooling. Urban with very high ratio between building height and street width, as well as the very dense settlement may have high waste heat from human activities. In Bogor, where only a few tall buildings are available, the dominant heat contributors might become from human (metabolic and non-metabolic) activities and road traffic. Fan and Sailor pointed out that road traffic contributed about 32% of heat emission while the human metabolic heat emission is only 8% [2].

Frequently, cities have warmer land's average temperature than its surrounding suburban and rural areas. The rapid development of built-up areas in Bogor, such as settlements, tall buildings for hotel, commerce, and/or offices, mainly alters the physical

characteristics of the land surface, from vegetation to non-vegetated areas. The replacement of green vegetated surfaces with non-vegetated and non-porous urban materials with high heat capacity and low solar reflectivities, such as concrete masses, asphalt roads and metal surfaces exhibit a high degree of thermal inertia [3]. These areas are characterized by a high level of absorption of solar radiation, with a greater capacity for thermal conductivity as compared to natural surfaces [4].

Within the built-up area, the glass-walled buildings may reflect the incoming short-wave solar radiation (sunlight), and consequently the surface, as well as the air temperature in the surrounding building may increase. In the cities, it is also quite common that emission from public traffic as well as private traffic may increase the GHG released to the atmosphere, then eventually increase the surface temperature. Some gasses that are emitted into the atmosphere will act as a greenhouse gas that is transparent to short-wave solar radiation and absorb long-wave radiation of the earth thus increasing global warming. Urban development can raise the local temperature of the city where the rate of temperature rise is proportional to the rate of urban development [5]. The increase of population also caused an increase of heat waste, mainly emitted from non-metabolic activities such as vehicles, personal waste, energy consumption and manufactures etc. This may affect local climate change especially air temperature directly and indirectly [6]. The temperature of the urban areas might be effectively managed and slightly modified by increasing the extent of GHG absorber or by reducing the source of heat gasses. The common strategy applied is by increasing the amounts of heat energy absorbed and stored in the vegetation. Vegetation would be a very effective way as it delivers several mechanisms of cooling simultaneously and it had been recognized as a very cheap way to implement the cooling strategy.

To spatially measure the spatial distribution of the heat emitter and heat absorber, it needs to develop a technique to derive land surface temperature quickly, consistently, accurately, comprehensively and with a reasonable cost. One technique that frequently applied is by using the remote sensing approaches. Traditionally, the land surface temperature is mapped by using interpolation technique using the data recorded by each national weather station. Interpolation method for sparsely stationed network had been a focus of many researchers, including the examination of geostatistics and deterministic approaches. This method will provide very rough map since the distances between climatology stations are very low. The different interpolation method can provide different accuracy and deviation.

Now, the availability of remotely sensed data recorded using thermal bands, coupling the available middle-infrared, near-infrared, as well as the visible bands, has given a very good prospect. There is no interpolation method required in this approach. The temperatures were derived from every grid of the data. The algorithm used by combining the thermal, near-infrared and red-band of Landsat data, the pixel-based temperature might be derived. On the LST estimation, the accuracy of LST estimation is mainly affected by the surface capability of emitting radiation. In many algorithms, the LST estimations are based on the assumption that the ground surface acts as a blackbody (emissivity equals one).

The Split-Window (SW) algorithm is the most commonly used, given that this algorithm removes the atmospheric effect and obtains the LST from the linear or nonlinear combination of the brightness temperatures of two adjacent channels centered at 11 and 12 μm . Wan [7] proposed a new refinement of the generalized SW algorithm added with a quadratic term of the difference amongst the brightness temperature of the adjacent thermal infrared channels. Remote sensing is a practical way to accomplish the monitoring and assessing the LST because it represents a relatively low-cost and rapid method to acquire up-to-date information over a large geographical area. The studies related to the land surface temperatures can also be found in Dash [8] and Akhoondzadeh and Saradjian [9] and Liu and Zhang [10]. The LST has been used as a key parameter in the physics of land surface processes. Other related studies on land surface temperature can be found in Liang *et al.* [11]; Zhang and He [12]. In order to control the urban development especially as a prevent of urban heat island in Bogor Municipality and also as a prediction of the land surface temperature, the main objective of the study was to estimate the land surface temperature (LST) based on the Landsat-8 OLI and TIRS imageries using Split-Window (SW) algorithm in Bogor Municipality.

2. Research Method

2.1 Study Area

Bogor Municipality is located in a hinterland area of the Capital City Jakarta that consisted of 6 districts and 68 villages, with area extent of about 11.694 ha. Geographically, the city is located between $06^{\circ}48'40''$ and $06^{\circ}46'22''$ East longitude; and between $6^{\circ}30'53''$ and $6^{\circ}40'08''$ South latitude (Figure 1). The city has been the main destination of many domestic tourists within the Jabodetabek, and the residential area of many people who are working in the Capital City Jakarta. Now, the city has been frequently selected by His Excellency President Joko Widodo as his second working office. Thus, Bogor municipality which is now becoming the center of various activities such as commerce, tourism, the residential and president palace has been chosen as a study site. Bogor Municipality has a high rate of population growth and development.

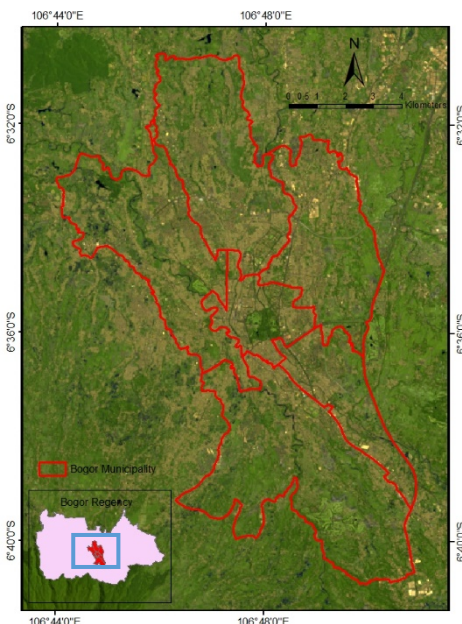


Figure 1. Study area research

2.2 The Supporting Data

The main data used are Digital Satellite Landsat-8 OLI (Operational Land Imager) imageries path 112-row 65; acquired on 13th September 2014. The bands used particularly red band (band 4), near infrared band (band 5), and Thermal Infrared Sensor (TIRS), namely band 10 and 11. The data was captured at approximately 10:00:37 a.m. local time. Landsat-8 provides metadata of the bands such as thermal constant and rescaling factor value that used for calculating the LST. Other primary data used to accomplish the study are surface temperature, land cover condition manually measured and observed at 5 Points. Although the Landsat-8 OLI recorded on 13th September 2014, while the ground measurement was done in March 2015, the difference between the temperature in March 2015 and in September 2014 in the day time is not significantly different. The land cover and land use within at the measurement points didn't change drastically.

2.3 Software, Hardware, and Tools Used

The spatial analysis was mainly performed using ArcMap 9.3 while the data processing of Landsat imageries were processed using ERDAS imagine 9.1. The processing platform was a personal computer with printing devices. For ground measurements, the tools used were Thermometer, GPS, and Camera.

2.4 Split-Window (SW) Algorithm

The theory underlying the technique of SW is that the radiance attenuation for atmospheric absorption is proportional to the radiance difference of simultaneous measurements at two different wavelengths [13]. The SW technique uses two TIR bands typically located in the atmospheric window between 10.30 and 12.50 μm . Furthermore, the following input required by the SW algorithm is brightness temperature, mean and difference in land surface emissivity (LSE) and water vapor.

The land surface temperature was calculated by converting the Digital Number (DN) of the two thermal bands (band 10, 11) into top of atmospheric radiance value, and then into the brightness temperature. Therefore, correction of the spectral emissivity has to be included. LSE was derived from NDVI threshold method by using the OLI bands 4, 5, and the emissivity values of TIR bands 10 and 11. In physical Atmospheric, the moisture content of the earth atmosphere is one of the most important parameters; it is hard to represent water vapor because of its space-time variation [14]. Water vapor content was the average of moisture for Bogor area. To obtain the water vapor content in September 2014 was to multiply the moisture by the ratio of water vapor content to the total standard atmospheric profiles for the tropical area [15]. The brightness temperature, mean and difference in LSE and water vapor content were used to calculate the LST. The formula is in equation-1 [16]:

$$\text{LST} = \text{BT}_{10} + C_1 (\text{BT}_{10} - \text{BT}_{11}) + C_2 (\text{BT}_{10} - \text{BT}_{11})^2 + C_0 + (C_3 + C_4 w) (1 - \varepsilon) + (C_5 + C_6 w) \Delta \varepsilon \quad (1)$$

where: LST is Land surface temperature (^0K); C_0 to C_6 are Split-window Coefficient values [17]; BT_{10} and BT_{11} are Brightness temperatures of band 10 and band 11 (in ^0K); ε is mean LSE of TIR bands; w is atmospheric water vapor content; and $\Delta \varepsilon$ is difference in LSE.

2.5 Ground Measurements

For validating the land surface temperature derived from the model in equation 1, the authors made ground measurements. Ground-based temperature measurements were taken in 13 days during March 2015 starting from 2nd March to 28th March. The measurement days were selected randomly, at the following specific date: 2nd, 4th, 7th, 9th, 11th, 14th, 16th, 18th, 21st, 23rd, 25th, 28th, and 30th. The locations of measurement were selected purposively at five different locations by considering the characteristics of land cover to be represented such as built-up, urban forest, rice field, housing and manufactured area. The temperature measurements were done between 10.00 – 12.00 am local time, which is the closest time to the Landsat-8 image captured. A total of five thermometers at measurement points were mounted at 1.5 m height in an open space that protected from solar radiation.

2.6 Data Analysis

To know the consistency and the relationship between these ground-based temperatures and the average of LSTs estimation, then the Pearson's correlation coefficients were derived. Besides, the deviation between the land's surface temperature estimate (LST) and the actual temperature were calculated by using mean deviation (MD) as in equation-2:

$$\text{MD} = \left\{ \frac{\left| \sum_{i=1}^n \frac{\hat{y} - y}{y} \right|}{n} \right\} \times 100\% \quad (2)$$

3. Results and Analysis

3.1 Land Surface Temperature Distribution

The input parameters to derive the LST of SW algorithm includes the brightness temperature of the two adjacent bands of the TIRS, mean and difference of emissivity which is an FVC can be estimated from the red and near-infrared reflectance of the OLI bands, and water vapor content. LST output portrayed that it varied from 301 to 322 Kelvin and converted into Celsius by subtracting 273.15. The spatial distribution of LST within the study area is shown in Figure 2. Across the entire study area, LST values increased from the outskirts towards the

inner urban areas, which ranged from 27°C to 50°C , with a mean of 37°C and a standard deviation of 3.67°C . The rise of surface temperature will affect to the increasing of air temperature especially in the urban areas (e.g., [18]). The LST pattern was found to be non-symmetrical but rather concentric, with high-temperature zones clustered towards the center of the study area. The areas with the lowest vegetation levels were corresponded to the land cover types of built-up area with the value of LST ranged from 40°C to 50°C . Conversely, high values of NDVI indicating the presence of green vegetation which mainly occurs, at the southern part of the study area. The corresponding land cover classes are farmland and grass area with the LST ranged from 27°C to 39°C . Some patches of high NDVI were also noticeable within the central region of the study area and corresponded to the urban forest area. The percentage area according to the temperature intervals was shown in Table 1.

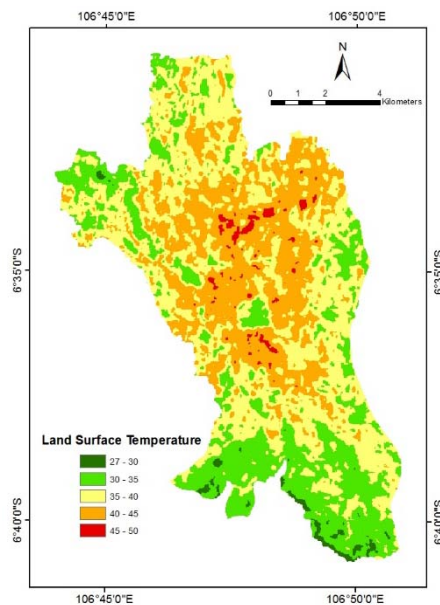


Figure 2. LST map

Table 1. LST percentage area

Class	Temperature Interval ($^{\circ}\text{C}$)	Area (Ha)	Proportion (%)
1	27 - 30	131.4	1.12
2	30 - 35	2,907.0	24.86
3	35 - 40	5,116.0	43.75
4	40 - 45	3,403.9	29.11
5	45 - 50	136.3	1.17
Total		11,694.6	100.00

The highest LST of more than 45°C is spread in the North and Center parts of Bogor with an area of 136.26 Ha. The smallest area of 131.4 Ha is varied from 27°C to 30°C . LST with the largest area of 5,116.05 Ha is varied from 35°C to 40°C . It has been largely demonstrated that cities with variable landscapes and climates can exhibit temperatures several degrees higher than their rural surroundings. The area with high LST is an area that dense with the settlements and roads (built-up). LST and land cover values were computed to understand further how LST interact with land cover parameters. The tabulated LST and land cover as shown in Table 2.

Table 2. Tabulated LST and land cover

No	Land Cover	Min	LST($^{\circ}$ C) Mean	Max
1	Urban Forest	27	34.5	42
2	Waterbody	28	36	44
3	Farmland	27	36	45
4	Grass	29	36.5	45
5	Built-up	29	39	49

The highest mean LST was found in built-up area having a temperature of 39°C , followed by the grass of 36.5°C , farmland and waterbody of 36°C , and the lowest temperature detected in the urban forest of 34.5°C . This implies that urban development has brought up LST by replacing natural vegetation with a non-evaporating and non-transpiring surface such as stone, metal, and concrete [19] [20].

3.2 Relationship between LST and Air Temperature

The correlation between LSTs and air temperature in the canopy layer was generally high, due to the transfer of thermal energy emitted from the surface to the atmosphere [21] [3]. The air temperature has a positive correlation with the LST at a day-time of day 1 and day 11 where the air temperature normally fluctuate less than LST across a given area during the day [22]. In general, the close relationship between LST and the air temperature has been shown to be valid [23] [24].

Pearson's correlation coefficients analysis (r) shows moderately high association with the value of 0.78 with the significant correlation of > 0.01 (1%) and mean deviation of 2.7%. Some research also shows the significant relationship during night-time measurement [25] [26]. Although there are differences between LST and air temperature, a moderate to high percentage of the air temperature can be estimated from the LST as indicated by coefficients of determination (R^2). The value R^2 obtained was in the range of 0.61 (Figure 3), this means that the variation of *in situ* temperature can be explained by the LST into 61%. In this case, the study area was limited only for Bogor Municipality, with the assumption that the ecological factor outside the study area was not considered.

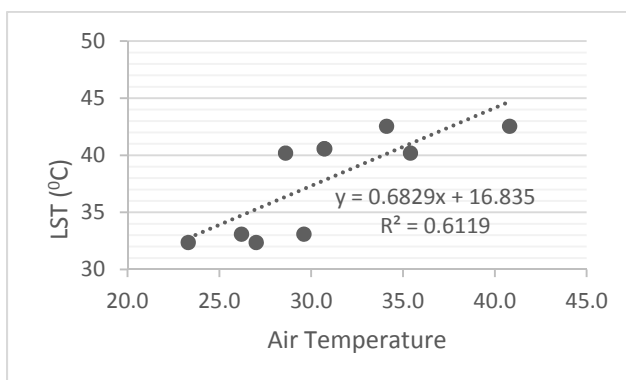


Figure 3. Relationship between LST and air temperature

By all means, we should not forget that the obtained relationship is based on the data of only two days, however complex, measurement campaigns. In the future, when using data of more measurements on days with similar environmental conditions to that of the investigated days, the result could be refined.

4. Conclusion

Landsat-8 TIRS sensor is capable of recording the radiant heat data on the earth's surface in the thermal infrared spectrum. The radiance heat information in the thermal spectrum is strongly influenced by the surface temperature and the object emissivity. As described by the Stefan-Boltzmann law, the total amount of emitted energy is directly proportional to the fourth power of the object's temperature. The split-window algorithm was used to determine the LST of an area. The land use changed in Bogor Municipality from the non-built area into built area has affected to the increasing of LST. The land surface temperature in Bogor Municipality can be estimated from the thermal sensors of satellite data exhibit by $r = 0.78$, with significant correlation 0.01 of the air temperature and mean deviation of 2.7. In the frame of this study, a data collection in different seasons could also be a new direction, which can provide a possibility to examine the specific seasonal features and enable their comparison.

Acknowledgments

Special thanks to the laboratory of Geophysics and Meteorology of Bogor Agricultural University for the equipment provided and Nils Nölke from Gottingen University for suggestions, corrections and comments for improvement of the original manuscript. It helps a lot for the revision of this paper.

References

- [1] Taha HG, Akbari H, Sailor D, Ritschard R. *Causes and Effect of Heat Islands: The Sensitivity of Urban Microclimates to Surface Parameters and Anthropogenic Heat*. Lawrence Berkeley Laboratory. Report No. 29864. Lawrence Berkeley, Davis California, USA. 1990.
- [2] Fan H, Sailor DJ. Modeling the Impacts of Anthropogenic Heating on the Urban Climate of Philadelphia: A Comparison of Implementations in Two Pbl Schemes. *Atmospheric Environment*. 2005; 39: 73–84.
- [3] Arrau CP and Pena MA. The Urban Heat Island (UHI) Effect. 2010. Available online at <http://www.urbanheatislands.com> (Accessed January 3rd, 2016).
- [4] Rose LA, Devadas MD. Analysis of and Surface Temperature and Land Use/ Land Cover Types Using Remote Sensing Imagery – A Case in Chennai City, India. Seventh International Conference on Urban Climate, Yokohama, Japan. 2009.
- [5] Fukui Y. A study on surface temperature patterns in the Tokyo metropolitan area using aster data. *Geoscience Journal*. 2003; 7: 343-346.
- [6] Mas'at A. 2008. The impact of development on climate variations in Jakarta. *BMKG Bulletin*. 2008; 4.
- [7] Wan Z. New refinements and validation of the collection-6 MODIS land-surface temperature/emissivity product. *Remote Sens. Environ.* 2014; 140: 36–45.
- [8] Dash, P. Land surface temperature and emissivity retrieval from satellite measurements. Dissertation. Institut für Meteorologie und Klimaforschung. ISSN 0947-8620. 2005.
- [9] Akhoondzadeh M, Saradjian MR. Comparison of Land Surface Temperature Mapping Using Modis and Aster Images in Semi-Arid Area. Remote Sensing Division, Surveying and Geomatics Dept., Faculty of Engineering, University of Tehran, Tehran, Iran. The International Archives of the Photogrammetry, Remote Sensing and Spatial Information Sciences. Vol. XXXVII. Part B8. Beijing 2008
- [10] Liu H, Zhang Shenglang Z. Land Surface Temperature Retrieval from the Medium Resolution Spectral Imager MERSI Thermal Data. *TELKOMNIKA Indonesian Journal of Electrical Engineering*. 2014; 12: 7287-7298
- [11] Liang S, Li X, Wang J. Advanced Remote Sensing: Terrestrial Information Extraction and Applications; Elsevier Science: Amsterdam, The Netherlands. 2012.
- [12] Zhang Z, He G. Generation of Landsat surface temperature product for China, 2000–2010. *Int. J. Remote Sens.* 2013; 34: 7369–7375.
- [13] Sobrino JA, Li ZL, Stoll MP, Becker F. Multi-channel and multi-angle algorithm for estimating sea and land surface temperature with ATSR data. *International Journal of Remote Sensing*. 1996; 17: 2089–2114.
- [14] Xin W, Xiaobo D, Shenglan Z. Retrieving Atmospheric Precipitable Water Vapor Using Artificial Neural Network Approach. *TELKOMNIKA Indonesian Journal of Electrical Engineering*. 2013; 11: 7174-7181.
- [15] Qin Z, Karniel A, Berliner P. A mono-window algorithm for retrieving land surface temperature from Landsat TM data and its application to the Israel-Egypt border region. *Int. J. Remote Sensing*. 2001; 22(18): 3719–3746.

- [16] Jimenez-Munoz JC, Sobrino JA, Skokovic D, Mattar C, Cristobal J. Land surface temperature retrieval methods from Landsat-8 thermal infrared sensor data. *IEEE Geosci. Remote Sens. Lett.* 2014; 11: 1840–1843.
- [17] Skokovic D, Sobrino JA, Jimenez-Munoz JC, Soria G, Julien Y, Mattar C, and Cristobal J. Calibration and Validation of Land Surface Temperature for Landsat 8 – TIRS Sensor. Land product Validation and Evolution, ESA/ESRIN Frascati (Italy). 2014: 6-9.
- [18] Cheng KS, Su YF, Kuo FT, Hung WC, Chiang JL. Assessing the effect of land cover changes on air temperature using remote sensing images – a pilot study in northern Taiwan. *Landscape Urban Plan.* 2008; 86: 85–96.
- [19] Lo CP, Quattrochi D, Luval J. Application of high-resolution thermal infrared remote sensing and GIS to assess the urban heat island effect. *International Journal of Remote Sensing.* 1997; 18:287–304.
- [20] Weng Q. A remote sensing-GIS evaluation of urban expansion and its impact on surface temperature in the Zhujiang Delta, China. *International Journal of Remote Sensing.* 2001; 22:1999–2014.
- [21] Nichol JE. A GIS-Based Approach to Microclimate Monitoring in Singapore's High-Rise Housing Estates. *Photogrammetric Engineering and Remote Sensing.* 1994; 60: 1225-1232.
- [22] EPA. 2009. Heat Island Compendium: Urban Heat Island Basics. Available online at: <http://www.epa.gov/heat-islands/heat-island-Compendium/UrbanHeatIslandBasics.pdf> (Accessed January 3rd, 2016)
- [23] Mostovoy GV, King RL, Reddy KR, Kakani VG, Filippova MG. Statistical estimation of daily maximum and minimum air temperatures from MODIS LST data over the state of Mississippi. *GISci. Remote Sens.* 2006; 43: 78–110.
- [24] Prihodko L, Goward SN. Estimation of air temperature from remotely sensed surface observations. *Remote Sens. Environ.* 1997; 60: 335–346.
- [25] Unger J, Gal T, Rakonczai J, Mucsi L, Szatmari J, Tobak J, Leeuwen B, and Fiala K. 2009. Air temperature versus surface temperature in urban environment. The seventh international conference on urban climate. Yokohama, Japan.
- [26] Li Z, Guo X, Dixon P, He Y. Applicability of Land Surface Temperature (LST) estimates from AVHRR satellite image composites in northern Canada. *Prairie Perspectives.* 2008; 11: 119.